OPEN

Hepatic Angiomyolipoma Mimicking Hepatocellular Carcinoma

Magnetic Resonance Imaging and Clinical Pathological Characteristics in 9 Cases

Chun-Ping Wang, MPhil, Hong-Yan Li, MD, Hong Wang, MD, Xiao-Dong Guo, MPhil, Chang-Chun Liu, MPhil, Shu-Hong Liu, MPhil, Xu-Dong Gao, MPhil, Jian-Hui Qu, MD, Ze Liu, MD, Xiu-Juan Chang, MPhil, Yin-Ying Lu, MD, Zhen Zeng, MD, Min Lou, MPhil, and Yong-Ping Yang, MD

Abstract: Hepatic angiomyolipoma (HAML) is a rare mesenchymal tumor of the liver with marked histological diversity. The present study was to review the magnetic resonance imaging (MRI) and clinical pathological features of HAML resembling hepatocellular carcinoma (HCC).

Nine patients who underwent surgical resection and had pathological diagnosis of HAML were retrospectively analyzed.

All of 9 patients (5 males and 4 females) had a solitary hepatic mass with a median size of 4 cm (from 1.4 cm to 15.3 cm). Seven cases were identified as incidental liver tumors during health screening and 2 patients were diagnosed for hepatic mass when visited hospitals with unspecific abdominal discomfort. Before resection, 6 cases were diagnosed as HCC on MRI. MRI on chemical shift imagings showed a large amount of lipids in 5 cases. The enhancement pattern of MRI was classified into 2 types: in 2 cases, lesions with small or no vessels that demonstrated prolonged enhancement (1 mixed subtype and 1 myomatous subtype) and in 7 cases, lesions with abundant central vessels that show rapid washout (3 mixed subtypes and 4 myomatous subtypes) in the portal venous/delayed phase. All patients underwent resection of hepatic tumor and no recurrence was observed during follow-up (range: 2–24 months) of median 10 months. By immunohistochemistry, the tumor cells demonstrated positive immunostaining for human melanoma black-45, smooth muscle actin, and CD34.

In conclusion, all of 9 patients with HAML presented with none or nonspecific clinical manifestations. The diagnosis of HAML relies on disease and immunohistochemistry, but not MRI due to its resemblance to HCC.

(*Medicine* 93(28):e194)

Abbreviations: AFP = α-fetoprotein, AML = angiomyolipoma, HAML = hepatic angiomyolipoma, HCC = hepatocellular carcinoma, HE = hematoxylin-eosin, HMB-45 = human melanoma black-45, MRI = magnetic resonance imaging, SMA = smooth muscle actin.

INTRODUCTION

Hepatic angiomyolipoma (HAML) is a rare, benign, liver mesenchymal neoplasm found in both males and females, and is most common in adult females.[1] However, it is a rare tumor with unpredictable behavior. Angiomyolipoma (AML) occurs most commonly in the kidneys. The liver represents the second most frequent site of involvement. The natural history of HAML in reported cases has not been clarified.

Moreover, the tumor is composed of blood vessels, smooth muscle cells, and a varying amount of fat, and because of the variation in predominance of these tissues it is histologically similar to AML found in the kidney. According to the line of differentiation and predominance of tissue components, these tumors have been classified into 4 subtypes: mixed, lipomatous ($\geq$70% fat), myomatous ($\leq$10% fat), and angiomatous. The most common subtype is the mixed subtype that comprises sheets of epithelioid muscle cells admixed with islands of adipocytes and abnormal vessels. The lipomatous and myomatous patterns are regarded as morphologic variations on a continuous spectrum, depending on the degree of adipose and myoid differentiation. The myomatous subtype is more common in the liver than in the kidney. Angiomatous AML contains many large thick-walled vessels and radiologically may be misinterpreted as an intrahepatic arterial aneurysm. According to the predominant component, growth pattern, cell type, and other features, the tumors are subcategorized into trabecular, pelioid, and inflammatory variants.

Patterns in imaging studies have resulted in diagnostic difficulty and misdiagnosis of the tumor as hepatocellular carcinoma (HCC) or hepatic adenocarcinoma in some cases.[2] However, recent advances in diagnostic imaging through a combination of ultrasonography, computed tomography, magnetic resonance imaging (MRI), and angiography, and specific immunohistochemical analysis of this tumor using human melanoma black-45 antigen (HMB-45) staining have resulted in accurate diagnosis and it is reported that accurate preoperative diagnosis can be currently made in 25% to 52% of cases.[3,4] The majority of these tumors are believed to be clinically benign during a mean follow-up period of 6.8 years. However, an increasing number of cases and aggressive changes including

Editor: Shizhang Ling.
Received: April 15, 2014; revised and accepted: September 25, 2014.
From the Center of Therapeutic Research for Liver Cancer (C-PW, H-YL, HW, X-DG, J-HQ, ZL, X-JC, Y-YL, ZZ, ML, Y-PY); Center of Pathology (X-DG, S-HL); and Center of Radiology (C-CL), 302 Military Hospital, Beijing, China.
Correspondence: Yong-Ping Yang, Center of Therapeutic Research for Liver Cancer, 302 Military Hospital, 100 Xi Si Huan Zhonglu, Beijing 100039, China (e-mail: yongpingyang@hotmail.com).
C-PW, H-YL, and HW contributed equally to the writing of this article.
This work was supported by the Military Special-Purpose Program (No. BWS11J074) and the Key Scientific and Technological Research Fund of the National Special-Purpose Program, China (No. 2013ZX10005002).
The authors have no conflicts of interest to disclose.

ISSN: 0025-7974
DOI: 10.1097/MD.0000000000000194

increase in size, recurrence after surgical resection, metastasis, and invasive growth pattern into the parenchyma and along the vessels have been reported.[5–9]

In this study, we summarize and discuss 9 HAML lesions identified in the 302 Military Hospital of China, focusing on MRI and both clinical and pathological characteristics of the tumors in order to achieve a better understanding of this disease and increase correct diagnosis.

MATERIALS AND METHODS

Patients

All 9 patients were diagnosed with HAML at the 302 Military Hospital of China between 2010 and 2012 according to MRI and disease after tumor resection. We summarize their gross features, MRI, and pathological features. The study met the requirements of the Declaration of Helsinki, and was approved by the Ethics Committee of the 302 Military Hospital.

Magnetic Resonance Imaging Scanning

MRI scanning was performed in all 9 patients using a GE HD × 1.5T scanner (General Electric Company, GE, USA) for plain scanning. Gadobenate dimeglumine (Gd-DTPA) was injected intravenously as a bolus, and a triphasic contrast-enhanced dynamic exploration during the arterial, portal venous, and delayed phases was performed. A torso-phased array surface coil, matrix: 256 to 320 × 256, layer thickness: 6 to 10 mm, layer spacing: 1 to 2 mm, and field of view: 34 to 40 × 40 cm was used. Patients breathed quietly with respiratory gating. T1-weighted images were obtained with a two-dimensional fast phase gradient reunion (FSPGR) imaging sequence and chemical shift imaging (in-out phase). T2-weighted images were obtained with respiratory triggering fat suppressed fast spin echo. Diffusion-weighted imagings were obtained at $B = 0$ s/mm and 800 s/mm^2. Multiphase contrast-enhanced scanning with a fat suppression liver acquisition with volume acceleration sequence of 64 to 92 layers was carried out. The injection speed of the magnetic resonance high-pressure syringe was 1.5 to 2.5 mL/s. The Gd-DTPA dose was 0.1 mmol/kg (body weight). Arterial phase scanning was performed 18 to 23 seconds after the first injection of Gd-DTPA, and then portal venous phase scanning was repeated 3 to 4 times (including coronal scanning). After 5 minutes, the delayed phase was performed in the axial scan.

Pathology and Immunohistochemistry

Protocols were as outlined below. Briefly, specimens were fixed using 10% formalin, dehydrated, paraffin-embedded, cut into 4 μm sections, stained with hematoxylin-eosin (HE) and observed under microscopy. Paraffin sections were evaluated for HMB-45, smooth muscle actin (SMA), S-100, CD34, CD117, hepatocytes, vimentin, epithelial membrane antigen, and Ki67 using streptavidin-peroxidase immunohistochemistry.[10,11] All antibodies and immunohistochemical kits were from Beijing Jinqiao Biological Technology Co, Ltd (Beijing, China). According to the proportion and distribution of vessels, smooth muscle and fat in the tumor as shown by Tsui et al,[12] the pathological types of HAML were classified into 4 subtypes: mixed subtype—this is the most common type and the tumors have cords of smooth muscle epithelial cells, islands of adipose tissue and abnormal vessels, and commonly include hematopoietic cells; lipomatous predominant subtype—these tumors have more than 70% fat tissue, epithelial cells, and short fusiform muscle forming a network structure in the adipose tissue; myomatous predominant subtype—these tumors are mainly composed of antral trabecular tissue with epithelial cells, and have <10% fat tissue; angiomatous predominant subtype—these tumors are composed of many large thick-walled vessels and fewer cell components.

RESULTS

Clinical Characteristics

Clinical characteristics of all of 9 cases are summarized in Table 1. The age of the 9 patients with HAML ranged from 39 to 62 years with a median of 50 years. Five patients were male and 4 were female. The hepatic mass was solitary, and the lesions ranged from 1.4 to 15.3 cm in diameter with a median diameter of 4 cm. Five lesions were located in the left lobe, 3 lesions in the right lobe, and 1 lesion was on the border between the left and right lobes. Physical examination showed no abnormalities in 7 cases and abdominal pain in 2 cases. Hematological and biochemical studies, including tumor markers such as α-fetoprotein (AFP), were normal. One of 2 hepatitis B surface antigen positive cases had cirrhosis. The remaining 7 cases had no history of liver disease. Tuberous sclerosis disease was not observed in these patients. Before hepatic tumor resection, one case was diagnosed with HAML. Six cases were diagnosed with HCC, and 2 cases were diagnosed with hepatic adenocarcinoma by MRI.

Microscopic and Immunohistochemical Features

The proportion of blood vessels, smooth muscle cells, and mature fat tissues in HAML varied significantly. Under microscopy, the proportions of these 3 tissues were similar in 4 cases, whereas the other five cases showed a predominance of fusiform or epithelioid muscle tissue. Based on Tsui et al[12] criteria, 4 lesions were classified as mixed subtype and 5 lesions were classified as myomatous subtype. The immunohistochemical study (Table 2) demonstrated that all cases were positive for HMB45, SMA, and CD34. Only 6 lesions showed positive staining for vimentin, and were negative for S-100, hepatocytes, and CD117. The Ki67 index was <20%.

MRI and Pathological Analysis

Numerous lipids were seen on chemical shift imagings in 5 cases (Figures 1–3). One of 4 cases with mixed subtype showed T1 slight hypointensity and T2 slight hyperintensity, whereas the other 3 lesions showed T1 hypointensity and T2 hyperintensity. All 4 cases showed large lipid components in chemical shift imagings (Figures 1 and 3). In 5 cases of myomatous predominant subtype, 2 cases showed T1 hypointensity and T2 slight hyperintensity, 2 cases showed T1 slight hypointensity and T2 slight hyperintensity, 1 case showed T1 hypointensity and T2 hyperintensity, and only 1 case showed focal lipid components in chemical shift imagings (Figure 2).

Contrast-enhanced scanning showed that mixed and myomatous subtype lesions were enhanced or significantly enhanced in the arterial phase. However, 2 types were observed in the portal venous phase and delayed phase: type I, lesions were obviously enhanced in the arterial phase and prolonged enhancement in the portal venous and delayed phases (1 mixed subtype and 1 myomatous subtype, Figures 1 and 2). Pathologically, the tumor contained less vascular tissue. Type II lesions were enhanced in the arterial phase, but followed by a rapid washout in the portal venous and delayed phases. The tumor was rich in blood vessels, mostly thin-walled sinusoidal

TABLE 1. Clinical Characteristics of All the 9 Patients With Hepatic Angiomyolipoma

Case No.	1	2	3	4	5	6	7	8	9
Age, y	53	53	50	62	55	41	46	39	49
Sex	F	M	M	M	M	F	F	M	F
HBsAg	Negative	Negative	Negative	Negative	Positive	Negative	Negative	Positive	Negative
Anti-HCV	Negative	Negative	Negative	Negative	Negative	Negative	Negative	Negative	Negative
Diabetes	No	No	No	No	No	No	No	No	No
BMI	19	22	23	28	25	22	21	26	24
Symptoms	Abdominal pain	Normal	Normal	Normal	Normal	Abdominal pain	Normal	Normal	Normal
AFP, ng/mL	1	3	4	4	5	5	14	14	3
ALT, U/L	12	12	13	8	16	10	8	17	5
Cirrhosis	No	No	No	No	No	No	No	Yes	No
Drinking history	Yes	Yes	Yes	No	Yes	No	No	Yes	No
Tumor location	Right lobe	Left lobe	Left lobe	Left lobe	Between left and right lobe	Left lobe	Right lobe	Right lobe	Left lobe
Tumor size, cm	8 × 10	15.3 × 10	1.4 × 1.4	4.0 × 3.5	3.4 × 3.7	4.8 × 5.2	3.1 × 2.7	1.7 × 1.7	6.5 × 4.9
Preoperative diagnosis	HCC	HCC	HCC	HAML	HCC	Adenocarcinoma	Adenocarcinoma	HCC	HCC
Follow-up, months	24	12	12	10	10	2	10	17	9
Recurrence	No	No	No	No	No	No	No	No	No

AFP = α-fetoprotein, ALT = alanine aminotransferase, BMI = body mass index, F = female, HAML = hepatic angiomyolipoma, HBsAg = hepatitis B surface antigen, HCC = hepatocellular carcinoma, HCV = hepatitis C virus, M = male.

blood vessels (3 mixed subtypes and 4 myomatous subtypes, Figures 3 and 4). Imaging showed pseudocapsule enhancement in 1 case of mixed subtype and 1 case of myomatous subtype.

MRI characteristics of HAML subtype from all 9 cases are summarized in Table 3. All of 9 patients underwent hepatic tumor resection and were followed up for 2 to 24 months (median: 10 months). No recurrences or metastases have been observed.

DISCUSSION

HAML, a member of the family of tumors, which show differentiation resembling perivascular epithelioid cells, was first described by Ishak[13] in 1976. Regardless of their location, the tumors in this family have mature fat, thick-walled poorly organized blood vessels and spindle-epithelioid myoid cells. HAML is a rare mesenchymal tumor of the liver. Tsui et al[12] described the morphologic variations of HAML, which reflect the variable lineage and degree of differentiation of myoid cells. The histologic patterns described in the literature include lipomatous, myomatous, angiomatous, trabecular, pelioid, inflammatory, and mixed pattern.[12] Although HAML has various subtypes or variants and mimics various hepatic neoplasms, it is recognized or suspected due to its morphologic parameters. Clues to the diagnosis of HAML include 3 characteristic components (blood vessels, smooth muscle, and fat tissue) and the diagnostic myoid component, which may exist in epithelioid, spindle, and intermediate forms. It has been speculated that the distinctive epithelioid cells are primitive mesenchymal cells with an ability to differentiate into both myoid and adipose cells. Immunohistochemically, these cells are strongly positive for HMB-45 and SMA.

HAML is very rare and its cause is still unclear. However, immunohistochemistry and electron microscopy showed a clonal proliferation. Vascular and smooth muscle components were monoclonal, whereas fat tissue composition was polyclonal. This suggested that the tumor cells derived from perivascular epithelioid cells were a type of primitive mesenchymal cells with multidifferentiation potential and could differentiate into vascular smooth muscle cells and adipocytes.[14]

It was reported that HAML occurs in adult women, mainly young and middle-aged women. There was no relationship with hormone levels, acyeterion history, or hepatitis.[2] The incidence of HAML in the present study was similar in males and females

TABLE 2. Pathological Characteristics of HAML Subtypes in All of 9 Cases

Cases	Postoperative HAML Subtypes	CD34	CD117	Hepatocyte	Vimentin	Ki67	SMA	HMB-45	S-100
1	Mixed subtype	++	Undetected	−	++	<5%	+	++	−
2	Mixed subtype	++	Undetected	−	Undetected	<20%	++	++	Undetected
3	Myomatous predominant subtype	+	−	−	+	<20%	+	+++	Undetected
4	Myomatous predominant subtype	++	−	−	−	<15%	+	+++	−
5	Mixed subtype	++	−	−	−	<20%	++	++	−
6	Myomatous predominant subtype	++	−	−	+	<5%	++	++	Undetected
7	Mixed subtype	+	−	−	+	<10%	+	++	−
8	Myomatous predominant subtype	++	−	−	++	<8%	+++	+	−
9	Myomatous predominant subtype	++	−	−	+	<3%	+++	++	−

HAML = hepatic angiomyolipoma, HMB-45 = human melanoma black-45, SMA = smooth muscle actin. The extent of positive staining was defined as follows: (-), negative; (+), weak; (++), moderate; (+++), strong.

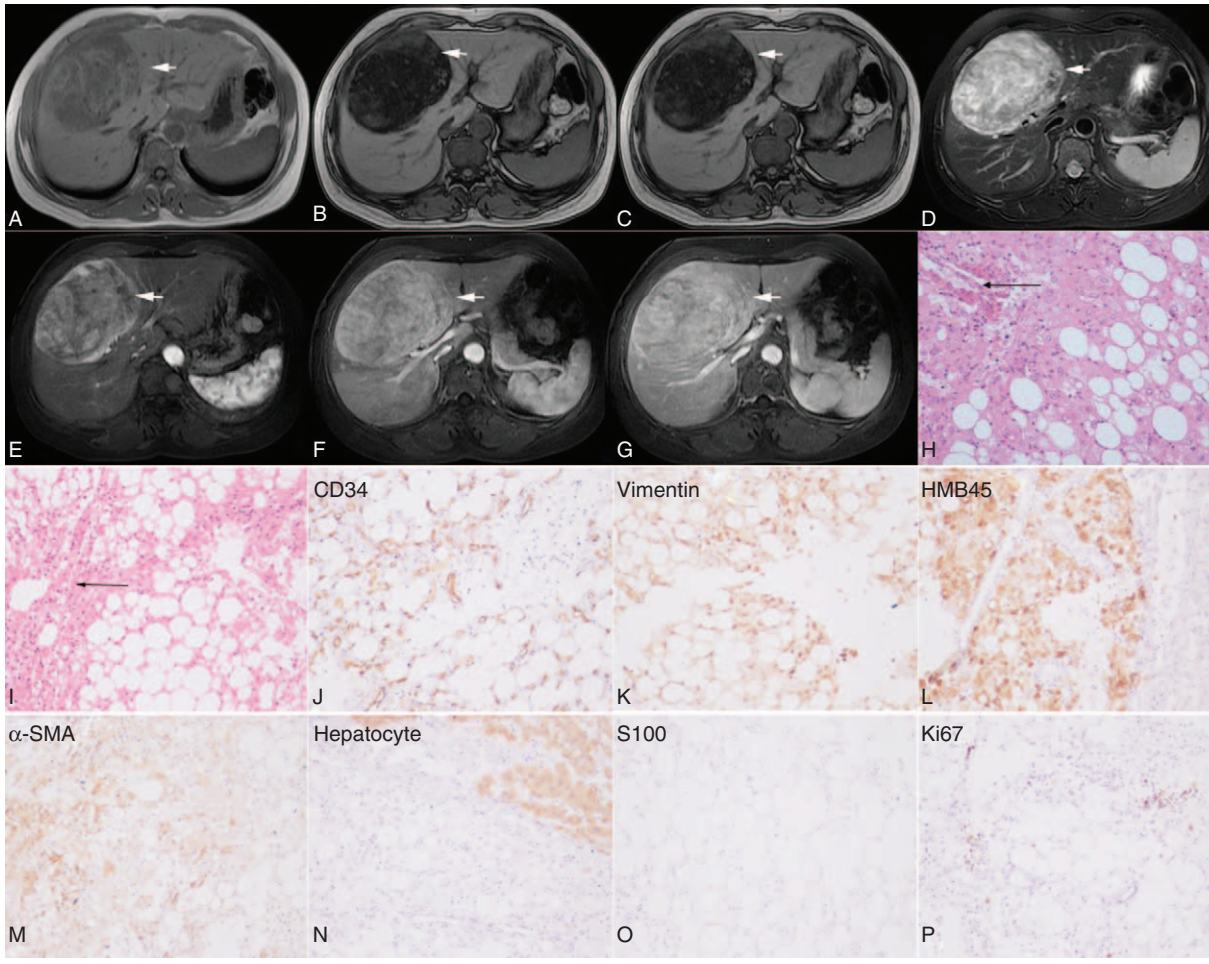

FIGURE 1. Histopathology and MRI of mixed type HAML: type I. Case 1: the pathological diagnosis was mixed type HAML. MRI: the lesion in the right liver lobe (arrow head) contained a large number of lipid components as seen on in-phase (A). The adipose tissue was shown as decreased signal intensity on out-of-phase image (B). The lesion showed T1 hypointensity (C) and T2 hyperintensity (D). Contrast-enhanced scanning showed obvious enhancement in the arterial phase (E), which was prolonged enhancement in the portal venous phase (F) and delayed phase (G). The peripheral pseudocapsule was annularly enhanced. Histolopathology (H and I, HE staining, ×200) showed the tumor included mature fat, blood vessels, and epithelioid-spindle cells. Thick-walled blood vessels (arrow) were seen in the tumor tissue. Immunohistochemical staining (×200): CD34 underlined the rich vascular channels, whereas the epithelioid-spindle cells were negative (J). The epithelioid-spindle cells were strongly positive staining for vimentin (K), HMB-45 (L), α-SMA (M), but were negative staining for hepatocyte (N) (but positive for liver tissues surrounding the tumor), S100 (O). Ki67 index was <5% (P). HE = hematoxylin-eosin.

due to the limited number of cases. The clinical manifestations of HAML were unremarkable, and 7 (77.78%) of the 9 patients had no obvious symptoms and 2 (22.22%) had abdominal pain. The majority of lesions were found on medical examination or when the patients were examined for other diseases. Liver function in these patients was not obviously abnormal and the level of AFP was normal. The patients did not have a history of cirrhosis. It was demonstrated that approximately 5% to 10% of cases have tuberous sclerosis syndrome and renal AML[12]; however, the patients in the present study did not have tuberous sclerosis, and this may be because of the limited number of cases.

In the present patient group, HAML lesions were solitary nodules without lobar preferences. It has been reported that these tumors vary in size from 0.1 to 36 cm. The pathological characteristics of HAML included mature fat cells, smooth muscle cells, and abnormal blood vessels visible under microscope. However, these 3 components varied in composition and distribution, and these tumors could easily be misdiagnosed as HCC, leiomyosarcoma, angiosarcoma, hepatic adenocarcinoma, lipoma, adipose-derived mesenchymal tumor, or hamartoma. It has been reported that the positive expression rate of HMB-45 in tumor-like smooth muscle cells was >95%, and the positive expression rates of other indices, such as SMA or vimentin, were >90%.[15,16] In our patients, the positive expression rates of HMB-45, SMA, and CD34 were all 100%, consistent with the composition of pathological tissues. In addition, the positive expression rate of vimentin was 66.6%, whereas S-100, hepatocytes, and CD117 were negative. Therefore, it was concluded that the positive expressions of HMB-45, SMA, and CD34 were specific markers for disease diagnosis. However, HAML can be identified in patients with liver metastasis from malignant melanoma, due to the positive expressions of HMB-45 and melan A in malignant melanoma.[17]

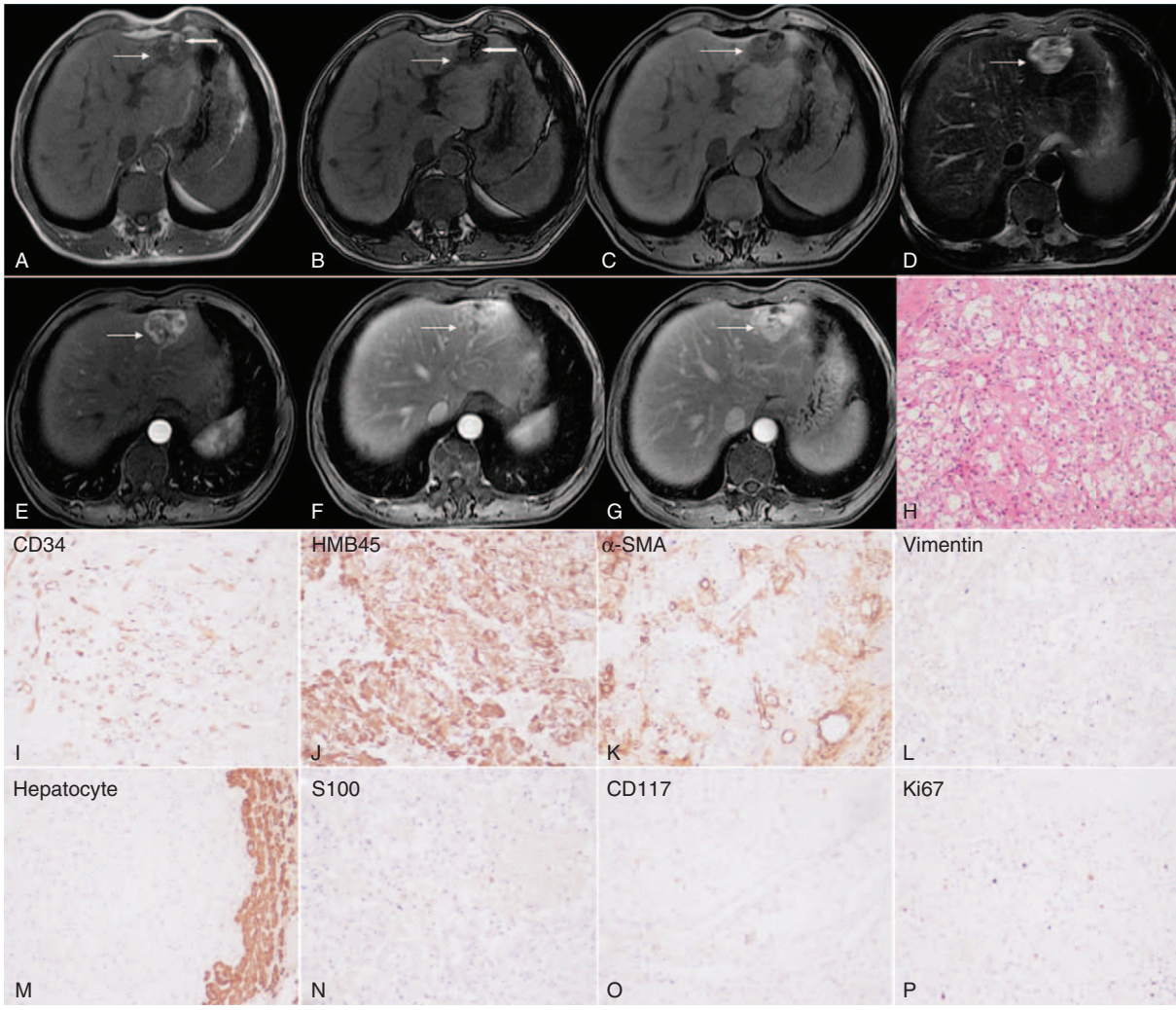

FIGURE 2. Histopathology and MRI of myomatous predominant HAML: type I. Case 4: the pathological diagnosis was myomatous predominant HAML. MRI: the lesion in the left lateral liver lobe was 4.0 cm × 3.5 cm in size (arrow) and a focal lipid component was seen on in-phase (A). The adipose tissue demonstrated decreased signal intensity on out-of-phase image (B). The lesion showed T1 hypointensity (C) and T2 hyperintensity (D). Contrast-enhanced scanning showed that the periphery of the lesion was annularly enhanced in the arterial phase (E) and obviously heterogeneously prolonged enhancement in the portal venous (F) and delayed phase (G). Tumor disorder showed predominance of epithelioid-spindle cells, with less vascular tissue (H; HE staining, ×200). Immunohistochemical staining (×200): CD34 underlined vascular channels (I). The epithelioid-spindle cells were strongly positive staining for HMB-45 (J), α-SMA (K), but were negative staining for vimentin (L), hepatocyte (M), S100 (N), and CD117 (O). Ki67 index was <15% (P). HE = hematoxylin-eosin.

Moreover, the Ki67 index was <20%, indicating that HAML was a benign tumor.

As the tumor composition and morphologic variation are different in HAML patients, it is difficult to form highly specific diagnostic criteria from imaging studies. According to the previously published studies,[1,18] MRI can reveal the imaging characteristics of mixed subtype HAML. Under contrast-enhanced scanning, all lesions were enhanced in the arterial phase and were prolonged enhancement in the portal venous phase and delayed phase. Myomatous subtype lesions tended to be enhanced in the arterial phase and followed by a rapid washout in the portal venous phase and delayed phase.[1,19] The 9 cases of HAML in this study were analyzed according to MRI and pathological analysis. The results demonstrated that mixed subtype and myomatous subtype lesions were enhanced or obviously enhanced in the arterial phase, similar to the findings in those previously reported.[1,18,19] However, 2 types were found in the portal venous phase and delayed phase. Type I in 2 cases, lesions with small or no vessels demonstrated obvious enhancement in the arterial phase and strengthened in the portal venous phase and delayed phase (1 mixed subtype and 1 myomatous subtype). Type II in 7 cases, lesions with abundant central vessels (mostly thin-walled sinusoidal vessels) showed enhancement in the arterial phase and followed by a rapid washout in the portal venous phase and delayed phase (3 mixed subtypes and 4 myomatous subtypes). These MRI features shown to be type II were similar to HCC, as the tumor tissue was rich in incomplete thin-walled sinusoidal vessels, poor vascular growth, and the contrast agent entered and exited quickly. Therefore, mixed subtype HAML did not show obvious

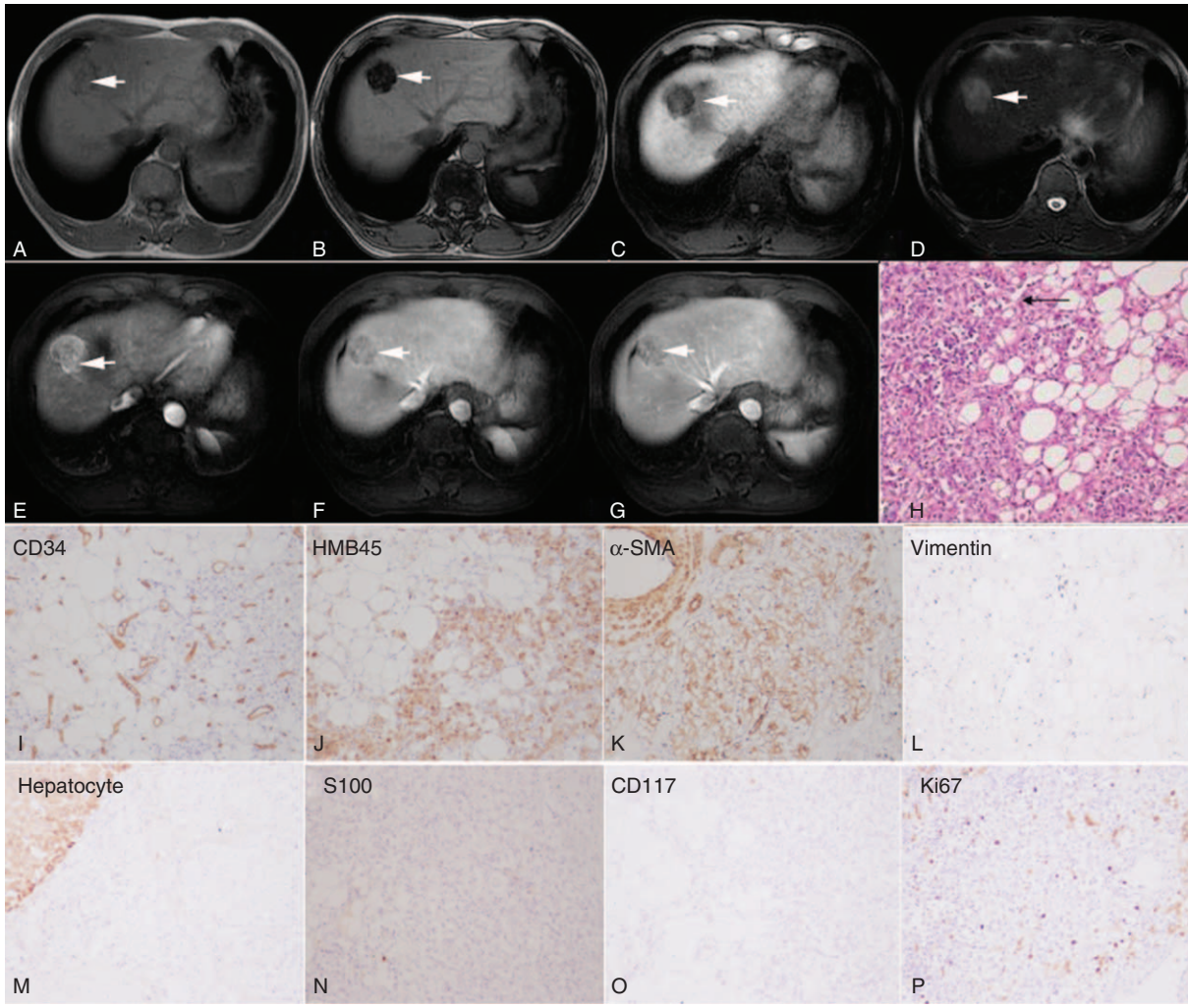

FIGURE 3. Histopathology and MRI of mixed type HAML: type II. Case 5: the pathological diagnosis was mixed type HAML. MRI: the lesion on the border between S4 and S8 (arrow head) contained a large number of lipid components as seen on in-phase (A). The adipose tissue demonstrated decreased signal intensity on out-of-phase image (B). The lesion showed T1 hypointensity (C) and T2 hyperintensity (D). Contrast-enhanced scanning showed a lesion with obvious enhancement in the arterial phase (E), followed washout in the portal venous phase (F) and delayed phase (G). The tumor tissue was rich in small thin-wall tortuous vessels (arrow; H). Immunohistochemical staining (×200): CD34 underlined the rich vascular channels (I). The epithelioid-spindle cells were strongly positive staining for HMB-45 (J), α-SMA (K), but were negative staining for vimentin (L), hepatocyte (M), S100 (N), and CD117 (O). Ki67 index was <20% (P).

enhancement in the arterial phase and was strengthened in the portal venous phase and delayed phase due to the varied disease. In addition, a small number of myomatous subtype lesions enhanced on MRI were shown to be type I, whereas more myomatous subtype lesions enhanced on MRI were shown to be type II. In this study, MRI characteristics of 3 cases of mixed subtype and 4 cases of myomatous subtype HAML were enhanced in the arterial phase and followed by a rapid washout in the portal venous and delayed phase, which were difficult to distinguish from HCC, similar to the findings of other researchers.[1,19]

How do we differentiate the diagnosis of HAML from HCC? Firstly, clinical history is very important. In asymptomatic patients, especially young or middle-aged women, with an incidentally identified large liver mass without surrounding invasion and metastasis, with no history of chronic hepatitis and who are AFP negative, a possible diagnosis of HAML should be considered. Secondly, in type I, using MRI for mixed subtype HAML, the diagnosis was relatively easy. However, in type II, the MRI characteristics of mixed subtype HAML showed fat tissues in the tumor, which is the key to HAML diagnosis.[1,18] The chemical shift imaging is useful, having higher sensitivity for the detection of intracellular lipids or dispersed foci of fat. Lipomatous lesions may be determined as hyperintensity on in-phase image and a relative decrease of signal intensity on out-of-phase image.[20,21] In this study, numerous lipid components were found in the tumors of 4 cases of mixed subtype HAML using magnetic resonance chemical shift imaging technique. However, these findings should be clarified in patients with HCC associated with steatosis. We treated a middle-aged male patient with chronic hepatitis B whose AFP was 24 ng/mL. The preoperative MRI characteristics were as follows: the lesion in the right liver lobe showed T1 hypointensity and T2 hyperintensity. The boundary was clear. The lesion

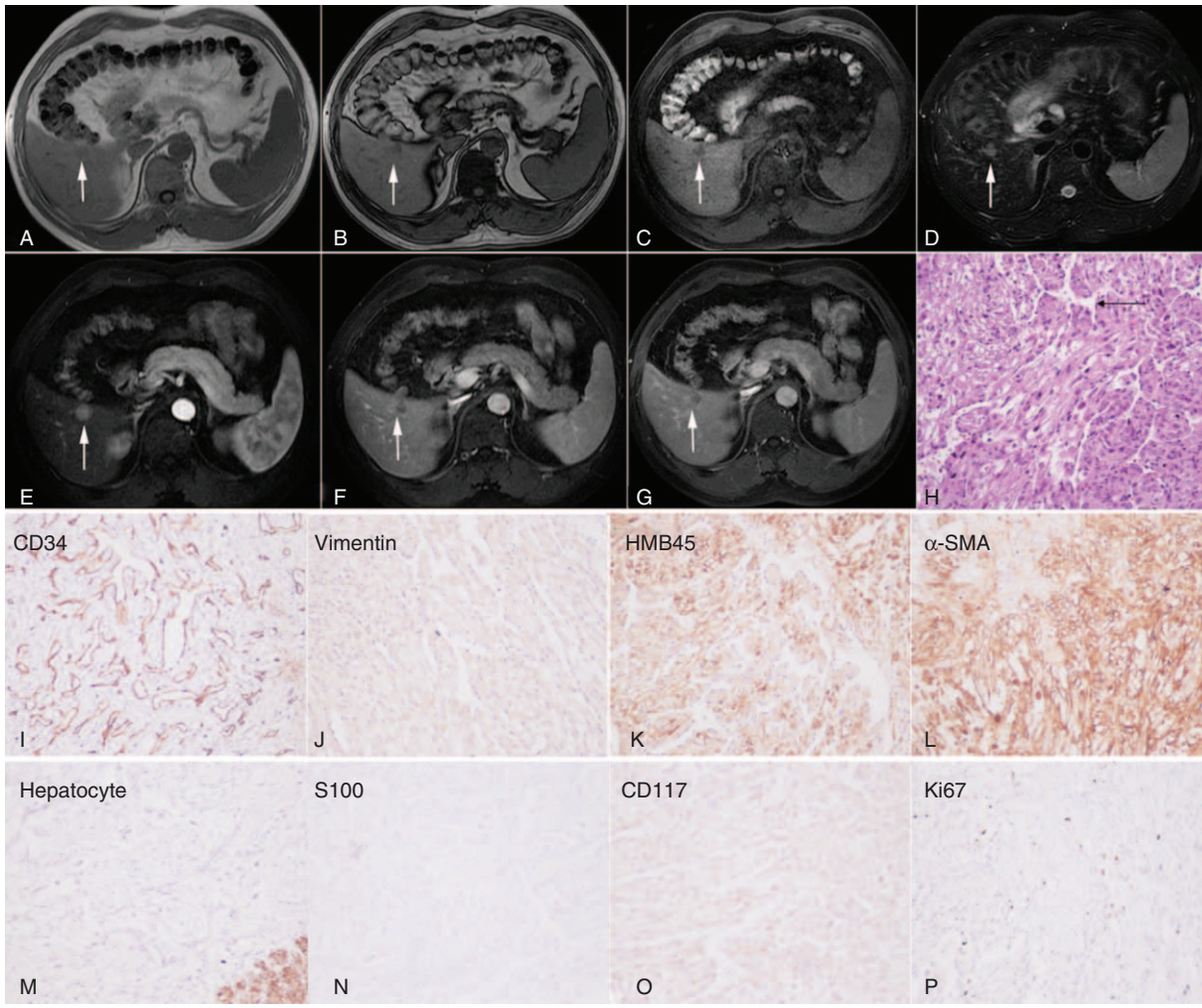

FIGURE 4. Histopathology and MRI of myomatous predominant HAML: type II. Case 8: the pathological diagnosis was myomatous predominant HAML. MRI: The lesion in the S5 liver lobe (arrow) was 17 mm in diameter and the chemical shift imagings showed no lipid components (A, B). The lesion showed T1 slight hypointensity (C) and T2 slight hyperintensity (D). Contrast-enhanced scanning showed a lesion with obvious enhancement in the arterial phase (E), followed washout in the portal venous phase (F) and delayed phase (G). Imaging showed pseudocapsule enhancement. The tumor was pathologically rich in blood vessels with mostly thin-walled sinusoidal blood vessels (arrow; H). Immunohistochemical staining ($\times$200): CD34 underlined the rich vascular channels (I). The epithelioid-spindle cells were strongly positive staining for vimentin (J), HMB-45 (K), α-SMA (L), but were negative staining for hepatocyte (M), S100 (N), and CD117 (O). Ki67 index was $<$8% (P).

contained a large number of lipid components as shown by double echo sequences. The lesion was approximately 8.5 $\times$ 7.1 cm in size. Contrast-enhanced scanning demonstrated that the lesion showed heterogeneous enhancement in the arterial phase, whereas the contrast agent showed washout in the portal venous phase and delayed phase. The peripheral pseudocapsule was annularly enhanced. Preoperative diagnosis was HAML, whereas HMB-45 based on postoperative pathological analysis was negative. Postoperative diagnosis was HCC (Figure 5). Thirdly, in myomatous subtype HAML, adipose tissue was rarely seen in fat suppression sequences. As MRI of myomatous subtype HAML is very similar to that of HCC, it is difficult to distinguish one from the other.[22,23] It has been reported that punctate, filiform, or thick curved blood vessels in the tumor are characteristic of myomatous subtype HAML on magnetic resonance images, which could distinguish between myomatous subtype HAML and HCC [14]. However, the correct judgment is dependent on experienced radiologists. Fourthly, pathological and immunohistochemical detection of positive HMB-45, SMA, and CD34 are necessary for the correct diagnosis. Liver biopsy is helpful in the preoperative diagnosis of angiomyolipoma,[24,25] but because of reduced quality and pathological diversity of puncture samples, the diagnostic accuracy of preoperative biopsy was not high, and was reported to range from 0% to 40%. Lastly, early surgery for HAML is preferred for 3 reasons: It is difficult to distinguish from HCC, and if conservative treatment is administered, it is possible to miss the diagnosis of HCC; the large tumor size could cause liver symptoms; and a very small number of patients may develop cancer and recurrent disease (5–9). Recent studies suggested that a high level of Ki67 or P53 expression, or P53 mutation in exon 7 may demonstrate the malignant potential of HAML.[26]

TABLE 3. Magnetic Resonance Imaging Characteristics of HAML Subtypes in All of 9 Cases

Cases	Preoperative MRI Diagnosis	Postoperative HAML Subtypes	MRI Characteristics
1	HCC	Mixed subtype	The lesion on the border between liver left and right lobes showed T1 hypointensity and T2 hyperintensity whose size was 11.6 × 8.6 × 1.9 cm. Lesions contained large lipid compositions from the chemical shift imagings. Contrast-enhanced scanning: obviously enhanced in the arterial phase and prolonged enhancement in the portal venous phase and delayed phase. Peripheral pseudocapsule was annular enhanced.
2	HCC	Mixed subtype	The lesion on liver left lateral lobe showed T1 hypointensity and T2 hyperintensity whose size was 15.3 × 10.0 cm. The chemical shift imagings showed heterogeneous lipid compositions. Contrast-enhanced scanning: the lesion showed heterogeneous enhancement in the arterial phase, followed washout in the portal venous phase and delayed phase. The tumor performed heterogeneous hypointense to liver. Tumor in left lateral lobe contained hypervascular with lipid tissue.
3	HCC	Myomatous predominant subtype	The lesion on liver left lateral lobe showed T1 hypointensity and T2 slight hyperintensity whose diameter was 1.4 cm. The boundary was clear. Contrast-enhanced scanning: the lesion was slightly enhanced in the arterial phase, followed washout in the portal venous phase and delayed phase.
4	HAML	Myomatous predominant subtype	The lesion on liver left lateral lobe showed T1 hypointensity and T2 hyperintensity whose size was 4.0 × 3.5 cm. The boundary was clear. Echo sequence showed obviously focal lipid composition. Contrast-enhanced scanning: the lesion showed peripheral annular enhancement on the arterial phase and strengthened center was heterogeneously enhanced. The tumor was more obviously heterogeneously strengthened on the portal venous and delayed periods, at the center of which spots and sound signal were hypointense.
5	HCC	Mixed subtype	The lesion on the border between S4 and S8 showed T1 hypointensity and T2 hyperintensity, containing a large number of lipid compositions whose size was approximately 3.4 × 3.7 cm. Contrast-enhanced scanning: the lesion was obviously enhanced on the arterial phase, followed washout in the portal venous phase and delayed phase.
6	Hepatic adenocarcinoma	Myomatous predominant subtype	The slightly convex lesion on the left lateral lobe showed T1 hypointensity and T2 slight hyperintensity whose size was 4.8 × 5.2 cm. Contrast-enhanced scanning: the lesion was obviously enhanced on the arterial phase and hypointense strip to liver. Lesion was still slightly enhanced on the venous phase and delayed phase and slightly hyperintense strip to liver.
7	Hepatic adenocarcinoma	Mixed subtype	The lesion on S5 showed T1 slight hypointensity and T2 slight hyperintensity and the boundary was clear, whose size was 3.1 × 2.7 cm. Lesions contained large lipid compositions from the chemical shift imagings. Contrast-enhanced scanning: the lesion was homogeneously enhanced on the arterial phase, followed washout in the portal venous phase and delayed phase.
8	HCC	Myomatous predominant subtype	The lesion on S5 showed small round T1 slight hypointensity and T2 slight hyperintensity. Contrast-enhanced scanning: the lesion was obviously enhanced on the arterial phase, followed washout on the portal venous phase and delayed phase. Pseudocapsule enhancement was detected in the tumor. The diameter was approximately 17 mm.
9	HCC	Myomatous predominant subtype	The lesion on the left lobe showed T1 slight hypointensity and T2 slight hyperintensity. Contrast-enhanced scanning: the lesion was obviously enhanced on the arterial phase, followed washout on the portal venous phase and delayed phase, whose size was 6.5 × 4.9 cm.

HAML = hepatic angiomyolipoma, HCC = hepatocellular carcinoma, MRI = magnetic resonance imaging.

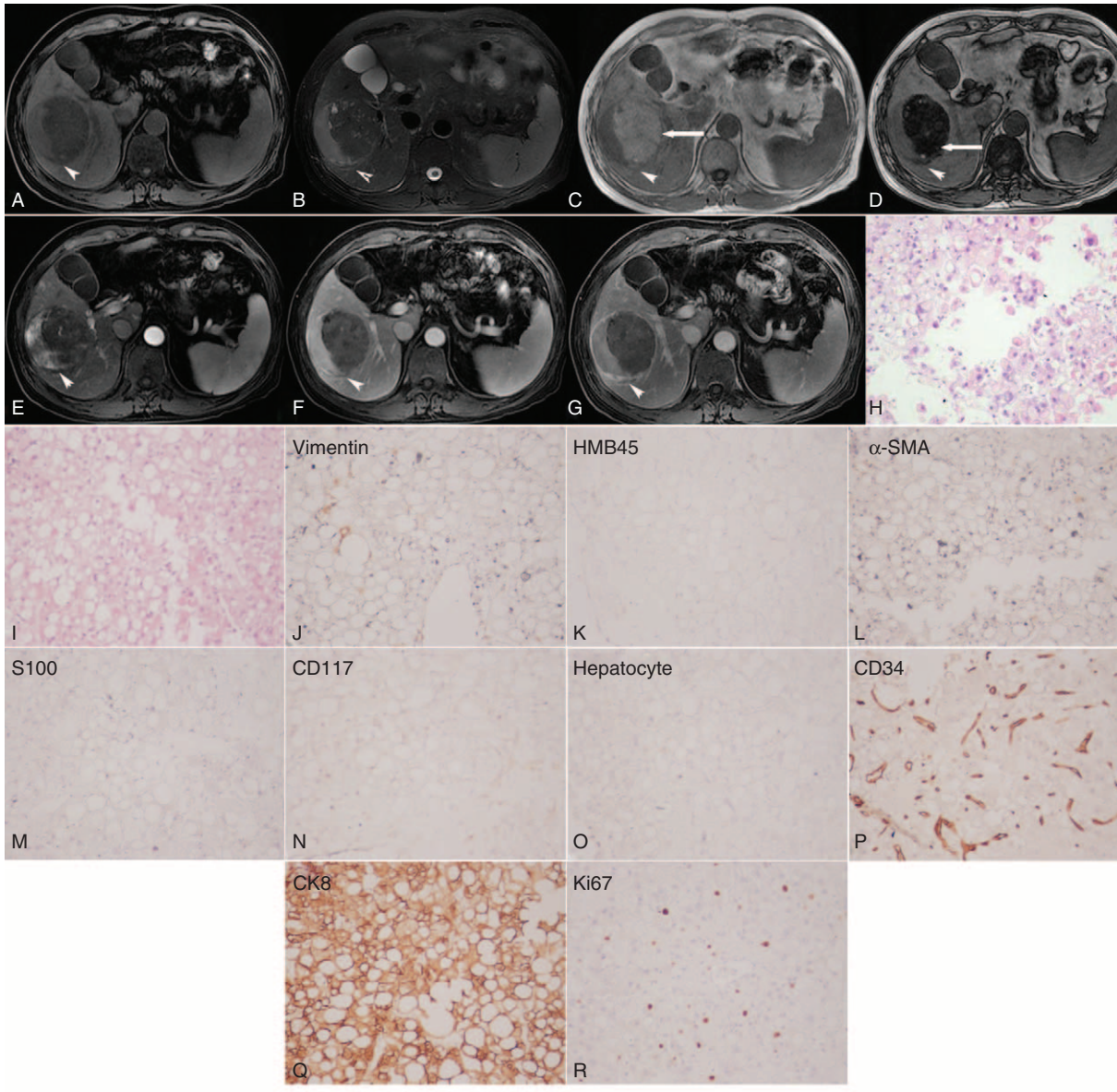

FIGURE 5. Histopathology and MRI of hepatocellular carcinoma with steatosis. In a 57-year-old male patient, preoperative MRI diagnosis was HAML, whereas postoperative pathological diagnosis was HCC. The lesion in the right liver lobe (arrow head) showed T1 hypointensity (A) and T2 hyperintensity (B). The boundary was clear. The lesion contained a large number of lipid components (arrow) as seen on chemical shift imagings (C, D). The lesion was approximately 8.5 × 7.1 cm in size. Contrast-enhanced scanning showed a lesion with heterogeneous enhancement in the arterial phase (E), followed washout in the portal venous phase (F) and delayed phase (G). The peripheral pseudocapsule was annularly enhanced. Histolopathology showed tumor cells had bizarre nuclei and mitotic figures were found (H and I; HE staining, ×200). Immunohistochemical staining (×200): The tumor cells were negative staining for vimentin (J), HMB-45 (K), α-SMA (L), S100 (M), and CD117 (N). Although tumor cells were negative staining for hepatocyte (O), these were strongly positive staining for CD34 (P) and CK8 (Q), and Ki67 index was about 30% (R). HE = hematoxylin-eosin.

REFERENCES

1. Kamimura K, Nomoto M, Aoyagi Y. Hepatic angiomyolipoma: diagnostic findings and management. *Int J Hepatol.* 2012;2012:410781.

2. Wang YR, Qiu FB, Li ZK. Zhang X. hepatic angiomyolipoma epidemiological features and experiences of diagnosis and treatment recent 23 years in China. *J Hepatopancreatobiliary Surg (Chinese).* 2012;24:183–191.

3. Ding GH, Liu Y, Wu MC, et al. Diagnosis and treatment of hepatic angiomyolipoma. *J Surg Oncol.* 2011;103:807–812.

4. Chang Z, Zhang JM, Ying JQ, et al. Characteristics and treatment strategy of hepatic angiomyolipoma: a series of 94 patients collected from four institutions. *J Gastrointestin Liver Dis.* 2011;20:65–69.

5. Nonomura A, Enomoto Y, Takeda M, et al. Angiomyolipoma of the liver: a reappraisal of morphological features and delineation of new

characteristic histological features from the clinicopathological findings of 55 tumours in 47 patients. *Histopathology.* 2012;61:863–880.

6. Croquet V, Pilette C, Aubé C, et al. Late recurrence of a hepatic angiomyolipoma. *Eur J Gastroenterol Hepatol.* 2000;12:579–582.
7. Rouquie D, Eggenspieler P, Algayres JP, et al. Malignant-like angiomyolipoma of the liver: report of one case and review of the literature. *Ann Chir.* 2006;131:338–341.
8. Nguyen TT, Gorman B, Shields D, et al. Malignant hepatic angiomyolipoma: report of a case and review of literature. *Am J Surg Pathol.* 2008;32:793–798.
9. Parfitt JR, Bella AJ, Izawa JI, et al. Malignant neoplasm of perivascular epithelioid cells of the liver. *Arch Pathol Lab Med.* 2006;130:1219–1222.
10. Shao Y, Zhong DR, Li XH. Differences in morphology and immunohistochemistry between hepatic angiomyolipoma and renal angiomyolipoma. *Zhonghua Yi Xue Za Zhi (Chinese).* 2003;83:1142–1145.
11. Wang XY, Wu ZQ. Theories and Techniques of Immunohistochemistry. In: Ji XL, Shi ZL, eds. *Diagnostic Immunohistochemistry.* Military Medical Science Press (*Chinese*), Beijing;1997:20–21.
12. Tsui WM, Colombari R, Portmann BC, et al. Hepatic angiomyolipoma: a clinicopathologic study of 30 cases and delineation of unusual morphologic variants. *Am J Surg Pathol.* 1999;23:34–48.
13. Ishak KG. Mesenchymal tumors of the liver. In: Okuda K, Peters RL, eds. Hepatocellular carcinoma. New York: John Wiley & Sons, 1976: 247–307.
14. Makhlouf HR, Remotti HE, Ishak KG. Expression of KIT (CD117) in angiomylipoma. *Am J Surg Pathol.* 2002;26:493–497.
15. Xu AM, Zhang SH, Zheng JM, et al. Pathological and molecular analysis of sporadic hepatic angiomyolipama. *C Human Pathol.* 2006;37:735–741.
16. Wang ZC, Huang XR, Ma JQ. Clinical and pathological analysis of hepatic angiomyolipoma. *J Basic Clin Oncol (Chinese).* 2007;20:51–53.
17. Liu YQ, Sun Y, Li ZW, et al. The value of biopsy in hepatic angiomyolipoma diagnosis. *Chin J Diagnostic Pathol (Chinese).* 2011;18:52–55.
18. Ye HY, Xie ZF, Gao YG, et al. Comparative analysis of MRI and pathology of hepatic angiomyolipoma. *Chin J Radiol (Chinese).* 2001;35:679–682.
19. Ji JS, Lu CY, Wang ZF, et al. Epithelioid angiomyolipoma of the liver: CT and MRI feature. *Abdom Imaging.* 2013;38:309–314.
20. Balci NC, Akinci A, Akun E, et al. Hepatic angiomyolipoma demonstration by out of phase MRI. *J Clin Imag.* 2002;26:418–420.
21. Martin J, Falco J, Donoso L, et al. Hepatic angiomyolipoma: value of proton (fat/water) chemical shift fast low angle shot (FLASH) MR imaging technique in detecting fatty tissue content. *Magn Reson Imaging.* 1995;13:903–906.
22. Lee SJ, Kim SY, Kim KW, et al. Hepatic angiomyolipoma with minimal fat, mimicking hepatocellular carcinoma. *Clin Mol Hepatol.* 2012;18:330–335.
23. Hwang I, Yu E, Cho KJ. Hepatic angiomyolipoma with variable histologic features: 8 cases resembling hepatocellular carcinoma or inflammatory pseudotumor. *Korean J Gastroenterol (Korean).* 2012;60:242–248.
24. Rimola J, Martín J, Puig J, et al. Hepatic angiomyolipoma: progressive changes in size and tumor composition. *Abdom Imaging.* 2003;28:665–667.
25. Cha I, Cartwright D, Guis M, et al. Angiomyolipoma of the liver in fine-needle aspiration biopsies: its distinction from hepatocellular carcinoma. *Cancer.* 1999;87:25–30.
26. Deng YF, Lin Q, Zhang SH, et al. Malignant angiomyolipoma in the liver: a case report with pathological and molecular analysis. *Pathol Res Pract.* 2008;204:911–918.